Baryon-Number Violation by Two Units and the Deuteron Lifetime

F. Oosterhof, B. Long, J. de Vries, R. G. E. Timmermans, and U. van Kolck

Phys. Rev. Lett. **122**, 172501 — Published 29 April 2019

DOI: 10.1103/PhysRevLett.122.172501

Baryon-number violation by two units and the deuteron lifetime

F. Oosterhof,[1] B. Long,[2] J. de Vries,[3,4] R. G. E. Timmermans,[1] and U. van Kolck[5,6]

[1] *Van Swinderen Institute for Particle Physics and Gravity, University of Groningen, 9747 AG Groningen, The Netherlands*

[2] *College of Physical Science and Technology, Sichuan University, Chengdu, Sichuan 610065, China*

[3] *Amherst Center for Fundamental Interactions, Department of Physics, University of Massachusetts Amherst, Amherst, Massachusetts 01003, USA*

[4] *RIKEN BNL Research Center, Brookhaven National Laboratory, Upton, New York 11973-5000, USA*

[5] *Institut de Physique Nucléaire, CNRS/IN2P3, Université Paris-Sud, Université Paris-Saclay, 91406 Orsay, France*

[6] *Department of Physics, University of Arizona, Tucson, Arizona 85721, USA*

(Dated: February 12, 2019)

We calculate the lifetime of the deuteron with dimension-nine quark operators that violate baryon number by two units. We construct an effective field theory for $|\Delta B| = 2$ interactions that give rise to neutron-antineutron (n-$\bar{n}$) oscillations and dinucleon decay within a consistent power counting. We calculate the ratio of the deuteron lifetime to the square of the n-$\bar{n}$ oscillation time up to next-to-leading order. Our result, which is analytical and has a quantified uncertainty, is smaller by a factor $\simeq 2.5$ than earlier estimates based on nuclear models, which impacts the indirect bound on the n-$\bar{n}$ oscillation time and future experiments. We discuss how combined measurements of n-$\bar{n}$ oscillations and deuteron decay can help to identify the sources of baryon-number violation.

At the classical level the Standard Model (SM) has two accidental global $U(1)$ symmetries associated with baryon-number (B) and lepton-number (L) conservation [1–3]. At the quantum level only $B-L$ is conserved, while $B+L$ is anomalous. Since it can be expected that all global symmetries are only approximate, it is plausible that beyond-the-SM (BSM) physics violates B, L, and $B-L$ separately. For instance, extending the SM with the only gauge-invariant dimension-five operator leads to violation of L by two units [1–3]. Additional B- and L-violating operators appear at the dimension-six level, while the first gauge-invariant operators that violate B by two units ($|\Delta B| = 2$) appear at dimension nine [4].

The best limits on B-violating interactions come from the observed stability of the proton. The limit on its lifetime translates into a scale $\Lambda_{|\Delta B|=1} \gtrsim 10^{13}$ TeV for grand unified theories [5]. Such energies are out of reach of colliders. However, models exist wherein B is only violated by two units and the proton is stable [6–8]. These interactions lead to the oscillation of neutral baryons into antibaryons, in analogy to strangeness-changing SM interactions that lead to kaon-antikaon oscillations. In particular, a neutron in a beam can oscillate into an antineutron [9] that annihilates with a nucleon in a target, producing several pions with a few hundred MeV of energy [10]. An ILL experiment sets a lower limit on the neutron-antineutron (n-$\bar{n}$) oscillation time of $\tau_{n\bar{n}} > 0.86 \cdot 10^8\,\mathrm{s} \simeq 2.7$ yr (90% C.L.) [11], which converts to a BSM scale $\Lambda_{|\Delta B|=2} \gtrsim 10^2$ TeV, within reach of future colliders. An experiment at the European Spallation Source can improve $\tau_{n\bar{n}}$ by two orders of magnitude [12], probing regions of parameter space relevant for the observed baryon asymmetry of the universe [13].

Apart from "in-vacuum" n-$\bar{n}$ oscillations, $|\Delta B| = 2$ interactions also induce the decay of otherwise stable nuclei. A bound neutron can oscillate inside the nucleus into an antineutron, which then annihilates with another nucleon. Since a neutron and an antineutron have very different potential energies, the typical nuclear lifetime is far greater than $\tau_{n\bar{n}}$ [4]. Alternatively, two nucleons can annihilate directly. If n-$\bar{n}$ oscillations are the dominant mechanism, one can calculate how the nuclear lifetime and $\tau_{n\bar{n}}$ are related. This relation was previously obtained from phenomenological models of the nuclear wavefunction and the nucleon-antinucleon potential [10], a procedure that suffers from unknown uncertainties.

In this letter, we improve the theory of $|\Delta B| = 2$ interactions in the simplest nucleus, the deuteron, with effective field theory (EFT). EFT allows for all interactions and processes consistent with the symmetries. Figure 1 shows the two classes of diagrams that represent deuteron decay. The left diagram shows a process that converts a neutron into an antineutron, which then annihilates with the proton. It includes "in-medium" modifications of the oscillation time [14]. The right diagram involves direct two-nucleon (NN) annihilation. We show that for most $|\Delta B| = 2$ sources we consider the deuteron decay rate is indeed dominated by free n-$\bar{n}$ oscillations contained in Fig. 1(a). We then calculate R_d, the ratio of the deuteron lifetime, Γ_d^{-1}, and $\tau_{n\bar{n}}^2$ up to next-to-leading order (NLO) in the systematic EFT expansion. We extract a bound on $\tau_{n\bar{n}}$ from the existing limit $\Gamma_d^{-1} > 1.18 \cdot 10^{31}$ yr (90% C.L.) obtained in the SNO experiment [15]. We argue that one can partially identify the fundamental $|\Delta B| = 2$ operators at the quark level from combined $\tau_{n\bar{n}}$ and Γ_d^{-1} data.

Central to our analysis are the gauge-invariant $|\Delta B| = 2$ operators. As each quark field has $B = 1/3$, operators with at least six quarks are required. Since we expect $\Lambda_{|\Delta B|=2}$ to lie well above the electroweak scale, we focus

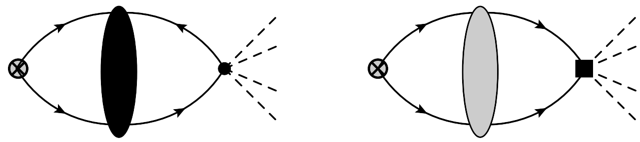

FIG. 1. The two classes of diagrams for deuteron decay. The crossed circle denotes the deuteron. Single lines with arrows to the right (left) denote (anti)nucleon propagators. In the left diagram, the blob depicts a one- or two-nucleon process that converts two nucleons into a nucleon and an antinucleon, and the circle their annihilation into a mesonic final state (dashed lines). In the right diagram, the blob depicts the propagation of two nucleons, and the square their direct annihilation into the same final states.

	Operator	Notation of Ref. [16]	Chiral irrep
$\mathcal{Q}_1$	$-\mathcal{D}_R\mathcal{D}_R\mathcal{D}_R^+\,T^{AAS}/4$	$\mathcal{O}^3_{RRR}$	$(\mathbf{1}_L,\mathbf{3}_R)$
$\mathcal{Q}_2$	$-\mathcal{D}_L\mathcal{D}_R\mathcal{D}_R^+\,T^{AAS}/4$	$\mathcal{O}^3_{LRR}$	$(\mathbf{1}_L,\mathbf{3}_R)$
$\mathcal{Q}_3$	$-\mathcal{D}_L\mathcal{D}_L\mathcal{D}_R^+\,T^{AAS}/4$	$\mathcal{O}^3_{LLR}$	$(\mathbf{1}_L,\mathbf{3}_R)$
$\mathcal{Q}_4$	$-\mathcal{D}_R^{33+}\,T^{SSS}/4$	$\left(\mathcal{O}^1_{RRR}+4\mathcal{O}^2_{RRR}\right)/5$	$(\mathbf{1}_L,\mathbf{7}_R)$

TABLE I. The independent $|\Delta B|=2$, SM gauge-invariant, dimension-nine operators with u and d quarks, and the irreducible chiral representations they belong to [19].

on the four operators [4, 16–18] that are invariant under the full SM gauge group $SU(3)_c\otimes SU(2)_L\otimes U(1)_Y$. At the QCD scale $\mu\sim 1$ GeV, we write

$$\mathcal{L}_{|\Delta B|=2}=\mathcal{C}_1\mathcal{Q}_1+\mathcal{C}_2\mathcal{Q}_2+\mathcal{C}_3\mathcal{Q}_3+\mathcal{C}_4\mathcal{Q}_4+\text{H.c.}\,, \quad (1)$$

where the six-quark operators $\mathcal{Q}_i$ are multiplied by complex Wilson coefficients $\mathcal{C}_i$ expected to scale as $\mathcal{O}(c_i\Lambda^{-5}_{|\Delta B|=2})$, with c_i dimensionless constants. The operators can be expressed via diquark fields [19] as

$$\begin{aligned}
&\mathcal{D}_{L,R}\equiv q^{iT}CP_{L,R}\,i\tau^2q^j\,,\quad \mathcal{D}^a_{L,R}\equiv q^{iT}CP_{L,R}\,i\tau^2\tau^aq^j\,,\\
&\mathcal{D}^{abc}_{L,R}\equiv\mathcal{D}^{\{a}_{L,R}\mathcal{D}^b_{L,R}\mathcal{D}^{c\}}_{L,R}-\frac{1}{5}\Big(\delta^{ab}\mathcal{D}^{\{d}_{L,R}\mathcal{D}^d_{L,R}\mathcal{D}^{c\}}_{L,R}\\
&\qquad+\delta^{ac}\mathcal{D}^{\{d}_{L,R}\mathcal{D}^b_{L,R}\mathcal{D}^{d\}}_{L,R}+\delta^{bc}\mathcal{D}^{\{a}_{L,R}\mathcal{D}^d_{L,R}\mathcal{D}^{d\}}_{L,R}\Big)\,, \quad (2)
\end{aligned}$$

where $q^i=(u^i\,d^i)^T$ is the quark doublet with color index i, C is the charge-conjugation matrix, $P_{L,R}$ are left- and right-handed projectors, τ^a $(a=1,2,3)$ are the Pauli isospin matrices, and $\{\}$ denotes symmetrization. Color singlets are formed by contracting the color indices suppressed on the left-hand side of Eq. (2) with the tensors

$$\begin{aligned}
T^{SSS}&\equiv\varepsilon_{ikm}\varepsilon_{jln}+\varepsilon_{ikn}\varepsilon_{jlm}+\varepsilon_{jkm}\varepsilon_{iln}+\varepsilon_{jkn}\varepsilon_{ilm}\,,\\
T^{AAS}&\equiv\varepsilon_{ikm}\varepsilon_{jln}+\varepsilon_{ikn}\varepsilon_{jlm}\,. \quad (3)
\end{aligned}$$

The resulting gauge-invariant operators are given in Table I, where $\tau^\pm=(\tau^1\pm i\tau^2)/2$.

Low-energy hadronic and nuclear observables such as $\tau_{n\bar n}$ and Γ_d^{-1} are difficult to calculate due to the breakdown of the perturbative expansion in the strong coupling constant. We use Chiral EFT (χEFT) [20, 21], the low-energy EFT of QCD with nucleons and pions as effective degrees of freedom. Pions play an important role as pseudo-Goldstone bosons of the spontaneously-broken, approximate $SU(2)_L\otimes SU(2)_R$ symmetry of QCD. In χEFT one can calculate observables at momenta $Q\lesssim m_\pi\simeq 140$ MeV, the pion mass, in an expansion in powers of Q/Λ_χ, where $\Lambda_\chi\sim 2\pi F_\pi\sim m_N$ is the chiral-symmetry-breaking scale, with $F_\pi\simeq 185$ MeV the pion decay constant and $m_N\simeq 940$ MeV the nucleon mass.

The first step towards the calculation of $|\Delta B|=2$ observables is to construct the chiral Lagrangian of QCD supplemented by Eq. (1). The EFT includes all chiral interactions that transform as the terms in this extended Lagrangian. Each term comes with a low-energy constant (LEC) that subsumes the nonperturbative QCD dynamics. These LECs have to be calculated with nonperturbative methods, preferably lattice QCD, or estimated, *e.g.* by naive dimensional analysis (NDA) [22].

In the single-baryon sector, we write the B-conserving Lagrangian for nonrelativistic (anti)nucleons $N=(p\,n)^T$ $(N^c=(p^c\,n^c)^T)$ interacting with pions π^a as

$$\begin{aligned}
\mathcal{L}^{(2)}_{\Delta B=0}&=N^\dagger\left(i\partial_0+\frac{\nabla^2}{2m_N}\right)N+N^{c\dagger}\left(i\partial_0+\frac{\nabla^2}{2m_N}\right)N^c\\
&+\frac{g_A}{F_\pi}\left(N^\dagger\sigma_k\tau^aN+N^{c\dagger}\sigma_k\tau^{aT}N^c\right)\nabla_k\pi^a\\
&-\frac{1}{2}\pi^a\left(\partial^2+m_\pi^2\right)\pi^a+\dots\,, \quad (4)
\end{aligned}$$

where σ_k $(k=1,2,3)$ are the Pauli spin matrices and $g_A\simeq 1.27$. Here and below the dots stand for terms that only contribute at higher orders in our calculation.

The chiral Lagrangian relevant for n-$\bar n$ oscillations has recently been constructed in Refs. [23–25], *viz.*

$$\mathcal{L}^{(2)}_{|\Delta B|=2}=-\delta m\,n^{c\dagger}n+\text{H.c.}+\dots\,, \quad (5)$$

where δm is a LEC that can be made real by a $U(1)$ transformation on the nucleon and antinucleon fields. Due to the chiral properties of the operators in Table I only $\mathcal{Q}_i$ with $i=1,2,3$ contribute at lowest orders [18], δm scaling as $\mathcal{O}(c_i\Lambda_\chi^2F_\pi^4/\Lambda^5_{|\Delta B|=2})$. The case $\mathcal{Q}_4$ is discussed below. The n-$\bar n$ oscillation time reads [23–25]

$$\tau_{n\bar n}=(\delta m)^{-1}\left[1+\mathcal{O}\left(m_\pi^2/\Lambda_\chi^2\right)\right]\,. \quad (6)$$

δm has recently been calculated in lattice QCD [26, 27].

To calculate deuteron decay we exploit the fact that the deuteron binding energy is only $B_d\simeq 2.225$ MeV. The fine-tuning represented by the small binding momentum $\kappa\equiv\sqrt{m_NB_d}\simeq 45$ MeV can be incorporated by assigning to NN LECs an enhanced scaling with respect to NDA [28]. The deuteron arises as a bound state when the leading NN interaction is iterated to all orders. Pion exchange between nucleons can be treated as subleading interactions in a perturbative expansion in Q/Λ_{NN} [29], where $\Lambda_{NN}\equiv 4\pi F_\pi^2/g_A^2m_N\sim F_\pi$ and $Q\sim m_\pi\sim\kappa$.

This scheme has been applied successfully to the electromagnetic form factors of the deuteron [30–33]. Since the nucleon-antinucleon ($N\bar{N}$) isospin-triplet $^3S_1$ scattering length $a_{\bar{n}p}$ has a natural value, similar enhancements of $N\bar{N}$ interactions are not necessary.

The B-conserving Lagrangian for NN and $N\bar{N}$ scattering we write as

$$\begin{aligned}\mathcal{L}^{(4)}_{\Delta B=0} = &-\left(C_0 + D_2 m_\pi^2\right)\left(N^T P_i N\right)^\dagger \left(N^T P_i N\right)\\ &+\frac{C_2}{8}\left[\left(N^T P_i N\right)^\dagger \left(N^T P_i (\overrightarrow{\nabla} - \overleftarrow{\nabla})^2 N\right) + \text{H.c.}\right]\\ &-H_0 (N^{cT}\tau^2 Y_i^a N)^\dagger (N^{cT}\tau^2 Y_i^a N) + \dots\ , \end{aligned} \tag{7}$$

where $P_i \equiv \sigma_2\sigma_i\tau^2/\sqrt{8}$ ($Y_i^a \equiv \sigma_2\sigma_i\tau^2\tau^a/2$) projects an NN ($N\bar{N}$) pair onto the isospin-singlet (triplet) $^3S_1$ state. The term with C_0 is the leading NN interaction, the real part of which scales as $\mathrm{Re}\, C_0 = \mathcal{O}(4\pi/m_N\kappa)$. One-pion exchange and one insertion of the subleading LECs $\mathrm{Re}\, C_2 \sim \mathrm{Re}\, D_2 = \mathcal{O}(4\pi/m_N\kappa^2\Lambda_{NN})$ appear at relative $\mathcal{O}(\kappa/\Lambda_{NN})$. Neglecting small imaginary parts discussed below, these LECs are determined from NN observables [29, 34], *e.g.*

$$C_0 = \frac{4\pi}{m_N(\kappa-\mu)} + \dots\ , \tag{8}$$

$$C_2 = \frac{4\pi}{m_N(\kappa-\mu)^2\Lambda_{NN}}\left[\frac{r_{np}\Lambda_{NN}}{2} - 1 + \frac{8\xi}{3} - 2\xi^2\right] + \dots,$$

where μ is the renormalization scale, $r_{np} \simeq 1.75$ fm [35] is the $^3S_1$ np effective range, and $\xi \equiv \kappa/m_\pi \simeq 0.32$. The LEC H_0 is the leading interaction in the $^3S_1$ $\bar{n}p$ channel, which is complex due to annihilation [36, 37]. Calculating the $^3S_1$ $\bar{n}p$ scattering amplitude and matching to the effective-range expansion, we obtain up to NLO

$$\begin{aligned} H_0 = &\frac{4\pi a_{\bar{n}p}}{m_N}\left[1 + \mu a_{\bar{n}p} + \frac{2(\mu - m_\pi)}{3\Lambda_{NN}}\right]\\ &+\frac{4\pi}{m_N\Lambda_{NN}^2}\left(\frac{4\mu}{9} - \frac{3m_\pi}{2}\right) + \dots \end{aligned}\tag{9}$$

We use the value $a_{\bar{n}p} = (0.44 - i\,0.96)$ fm obtained with a chiral potential [38, 39] fitted to state-of-the-art $N\bar{N}$ partial-wave amplitudes [40, 41]. The natural size of $a_{\bar{n}p}$ justifies the assignment $H_0 = \mathcal{O}(4\pi/m_N\Lambda_{NN})$ and the use of perturbation theory.

The presence of $|\Delta B| = 2$ interactions has two consequences. First, the B-conserving LECs get imaginary parts because two nucleons can now annihilate. The imaginary part is strongly suppressed, since it requires two $|\Delta B| = 2$ insertions; for example, $\mathrm{Im}\, C_0 = \mathcal{O}(\delta m^2\Lambda_\chi^2/\kappa^2\Lambda_{NN}^4)$, where we account for a $(\Lambda_{NN}/\kappa)^2$ enhancement due to renormalization by LO NN scattering on both sides of the vertex [28, 30]. Second, we need to consider the $NN \leftrightarrow N\bar{N}$ interactions

$$\mathcal{L}^{(4)}_{|\Delta B|=2} = i\tilde{B}_0\left[\left(N^T P_i N\right)^\dagger (N^{cT}\tau^2 Y_i^- N) - \text{H.c.}\right] + \dots\ , \tag{10}$$

where $\tilde{B}_0$ is a complex LEC. The NN interaction enhances it over NDA, $\tilde{B}_0 = \mathcal{O}(4\pi\,\delta m/\kappa\Lambda_{NN}^2)$, and implies that $\mathrm{Im}\,\tilde{B}_0/C_0 \propto (\kappa-\mu)\,\mathrm{Im}\,\tilde{B}_0$ is μ-independent, which becomes important below. Some interactions are further enhanced thanks to the one-body character of δm. For example, we find $\mathrm{Re}\,\tilde{B}_0 = \mathcal{O}(4\pi\,\delta m/\kappa^2\Lambda_{NN})$: requiring the NN and $N\bar{N}$ scattering amplitudes to be independent of the renormalization scale leads to a renormalization-group equation whose solution is

$$\mathrm{Re}\,\tilde{B}_0 = -m_N\delta m\,\mathrm{Re}\, C_2/\sqrt{2} + \dots \tag{11}$$

The mesonic final states in Fig. 1 contain hard pions with energies outside of the regime of χEFT. Instead of directly calculating deuteron-decay diagrams we determine the imaginary part of the pole of the deuteron propagator. The hard pions then only appear as intermediate states that can be integrated out. Following Ref. [30], we write the propagator for a deuteron with four-momentum $p^\mu = (2m_N + \vec{p}^{\,2}/4m_N + \bar{E} + \dots, \vec{p})$ in terms of the irreducible two-point function $\Sigma(\bar{E})$, which contains all diagrams that do not fall apart when cutting any $\mathrm{Re}\, C_0$ vertex, and expand around B_d, *i.e.*

$$G(\bar{E}) = \frac{\Sigma(\bar{E})}{1 + i\,\mathrm{Re}(C_0)\,\Sigma(\bar{E})} = \frac{iZ_d}{\bar{E} + B_d + i\Gamma_d/2} + \dots\ , \tag{12}$$

where the wavefunction renormalization Z_d is real and

$$\Gamma_d = \left.\frac{2\,\mathrm{Im}(i\Sigma(\bar{E}))}{\mathrm{Re}(\mathrm{d}i\Sigma(\bar{E})/\mathrm{d}\bar{E})}\right|_{\bar{E}=-B_d} + \dots \tag{13}$$

is the deuteron decay rate. Up to NLO [30],

$$\begin{aligned}\mathrm{Re}\left(\frac{\mathrm{d}i\Sigma(\bar{E})}{\mathrm{d}\bar{E}}\right)\bigg|_{\bar{E}=-B_d} &= \frac{m_N^2}{8\pi\kappa}\\ \times\bigg\{1 &+ \frac{m_N}{2\pi}(\kappa-\mu)\left[C_2\kappa(\mu-2\kappa) + D_2 m_\pi^2\right]\\ &+\frac{2}{\Lambda_{NN}}\left(\kappa - \mu + \frac{m_\pi}{1+2\xi}\right)\bigg\}\ . \end{aligned}\tag{14}$$

Figure 2 shows diagrams that give nonvanishing contributions to $\mathrm{Im}(i\Sigma(\bar{E}))$ up to NLO. We power-count diagrams with the following rules [28, 30]: $Q^5/(4\pi m_N)$ for each loop integral, m_N/Q^2 for each nucleon propagator, $1/Q^2$ for each pion propagator, and the product of the LECs appearing in each diagram. The dominant contribution to deuteron decay is due to diagram 2(a), which is $\mathcal{O}\left(\delta m^2 m_N^2/\kappa^2\right)$. A diagram with two δm insertions but no $N\bar{N}$ vertex is real and does not contribute to $\mathrm{Im}(i\Sigma)$. Diagrams 2(b,c,d,e,f) are $\mathcal{O}(\kappa/\Lambda_{NN})$ relative to 2(a) and give NLO corrections. Diagrams 2(b,c,d) are similar to 2(a) but involve an additional insertion of a subleading NN vertex (C_2 or D_2), a B-conserving pion exchange, or the leading $N\bar{N}$ vertex H_0. Diagrams 2(a,b,c,d) come from the left diagram in Fig. 1; they depend solely on δm and are directly related to the free n-$\bar{n}$ transition. Diagrams 2(e,f) are a mixture of both diagrams in Fig. 1.

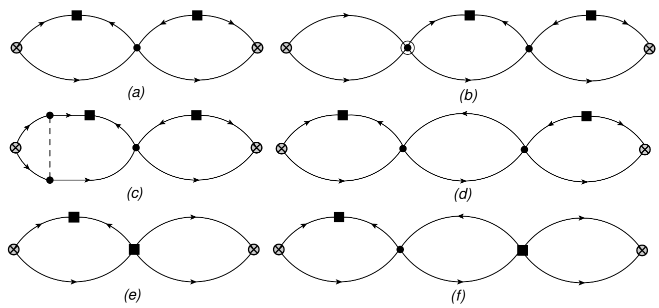

FIG. 2. Diagrams that contribute to $\mathrm{Im}(i\Sigma)$ up to NLO. Circles denote g_A or H_0 vertices, the circled circle denotes C_2 or D_2, and squares denote $|\Delta B| = 2$ vertices. The dashed line represents a pion. Only one ordering per diagram is shown.

They are proportional to, respectively, $\mathrm{Im}\,\tilde{B}_0$ and $\mathrm{Re}\,\tilde{B}_0$, the latter being related to δm by Eq. (11). From these diagrams we obtain

$$\begin{aligned}\mathrm{Im}(i\Sigma(-B_d)) = &-\left(\frac{m_N^2\delta m}{8\pi\kappa}\right)^2 \mathrm{Im}\,H_0 \\ &\times\Bigg\{1+\frac{m_N}{2\pi}(\kappa-\mu)\left[C_2\kappa(\mu-2\kappa)+D_2m_\pi^2\right] \\ &+\frac{8}{3\Lambda_{NN}}\left(\kappa-\mu+\frac{m_\pi}{1+2\xi}\right)+\frac{m_N}{2\pi}(\kappa-\mu)\,\mathrm{Re}\,H_0 \\ &-\frac{2\sqrt{2}\,\kappa(\kappa-\mu)}{m_N\delta m}\left[\frac{\mathrm{Im}\,\tilde{B}_0}{\mathrm{Im}\,H_0}+\frac{m_N}{4\pi}(\kappa-\mu)\,\mathrm{Re}\,\tilde{B}_0\right]\Bigg\}\,. \end{aligned} \tag{15}$$

The deuteron decay rate up to NLO is then

$$\begin{aligned}\Gamma_d = &-\frac{m_N}{\kappa\tau_{n\bar{n}}^2}\mathrm{Im}\,a_{\bar{n}p}\Bigg[1+\kappa\Bigg(r_{np}+2\,\mathrm{Re}\,a_{\bar{n}p} \\ &-\frac{g_A^2m_N}{3\pi F_\pi^2}\frac{2-2\xi-5\xi^2+6\xi^3}{1+2\xi}-\frac{(\kappa-\mu)\,\mathrm{Im}\,\tilde{B}_0}{\sqrt{2}\pi\,\delta m\,\mathrm{Im}\,a_{\bar{n}p}}\Bigg)\Bigg]\,. \end{aligned} \tag{16}$$

This result is independent of the renormalization scale, as it should be. It relates Γ_d to $\tau_{n\bar{n}}$ through known quantities and one unknown NLO constant $(\kappa-\mu)\,\mathrm{Im}\,\tilde{B}_0$, encoded in the ratio $R_d \equiv \Gamma_d^{-1}/\tau_{n\bar{n}}^2$. Numerically we find

$$\begin{aligned}R_d &= -\left[\frac{m_N}{\kappa}\mathrm{Im}\,a_{\bar{n}p}\;(1+0.40+0.20-0.13\pm 0.4)\right]^{-1} \\ &= (1.1\pm 0.3)\cdot 10^{22}\,\mathrm{s}^{-1}\,. \end{aligned} \tag{17}$$

The NLO corrections from known LECs affect the result by roughly 50% and are dominated by the effective-range correction. We account for the unknown value of $\mathrm{Im}\,\tilde{B}_0$ as an uncertainty of the same size as the effective-range correction. The explicit pion contributions amount to only 13%. The limit $m_\pi \to \infty$ recovers the result of Pionless EFT [36], where pions are integrated out and $\mathrm{Im}\,\tilde{B}_0$ absorbs the surviving pion term. Use of an auxiliary dibaryon field [36] automatically accounts for the enhancement of Eq. (11).

Our central value for R_d is smaller by a factor $\simeq 2.5$ than the often-used result from Ref. [42] based on

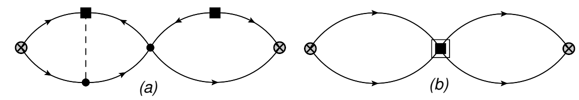

FIG. 3. Selected contributions to $\mathrm{Im}(i\Sigma)$ beyond NLO. The square-in-square denotes $\mathrm{Im}\,C_0$. Other notation as in Fig. 2.

nuclear models for the nucleon-(anti)nucleon interactions. We have checked that when the expressions from Refs. [42, 43] are applied to a zero-range potential we recover our LO term in Eq. (17). The difference therefore stems from the smaller $\mathrm{Im}\,a_{\bar{n}p}$ [44] of the $N\bar{N}$ potentials of Ref. [42], and from corrections to the zero-range limit. The diagrammatic approaches of Refs. [45, 46] also reduce to our LO for a zero-range potential. (Reference [47] disagrees from these results by a factor of 2.)

Our result is based on a systematic and improvable framework for all interactions, and we showed that NLO corrections are significant but of the expected size. In addition, we have used an up-to-date $\bar{n}p$ scattering length [39]. We therefore propose to use Eq. (17) in comparisons of deuteron stability and n-$\bar{n}$ oscillation beam experiments. Taking the largest value of R_d allowed by Eq. (17), the SNO limit on Γ_d^{-1} [15] gives

$$\tau_{n\bar{n}} = 1/\sqrt{R_d\Gamma_d} > 5.1\,\mathrm{yr} = 1.6\cdot 10^8\,\mathrm{s}\,, \tag{18}$$

about a factor two stronger than the direct ILL limit.

At higher orders we find some of the nuclear effects discussed in the literature, two examples being shown in Fig. 3. Diagram 3(a) can be seen as an "in-medium" modification of the n-$\bar{n}$ oscillation [14], due to the emission/absorption of pions in the n-$\bar{n}$ transition required by chiral symmetry and contained in the dots of Eq. (5). It is nominally of relative $\mathcal{O}(\kappa^2/\Lambda_{NN}m_N)$, but it actually vanishes. Corrections of this type should, therefore, be no larger than about 5%, to be compared with the 25-30% estimated for heavier nuclei in Ref. [48]. The effect of direct two-nucleon annihilation [18], the right diagram in Fig. 1, is represented by diagram 3(b). It is proportional to the absorptive part of NN interactions, $\mathrm{Im}\,C_0$, and appears at next-to-next-to-leading order ($\mathrm{N^2LO}$), $\mathcal{O}(\kappa^2/\Lambda_{NN}^2)$.

So far we have not discussed the operator $\mathcal{Q}_4$. Since it belongs to the $(\mathbf{1}_L, \mathbf{7}_R)$ irrep it can only contribute to $\tau_{n\bar{n}}^{-1}$ if additional sources of isospin violation are included. The lowest-order contribution to $\tau_{n\bar{n}}^{-1}$ involves two insertions of the charge, leading to a suppression of $\alpha_{em}/4\pi \sim \mathcal{O}(m_\pi^3/\Lambda_\chi^3)$ with respect to δm, where α_{em} is the fine-structure constant. $\mathrm{Im}\,C_0$ induced by $\mathcal{C}_4$ does not require the inclusion of extra isospin violation. For the case in which deuteron decay is dominated by $\mathcal{Q}_4$, *i.e.* $c_4 \gg c_{1,2,3}$, the imaginary part of diagram 3(b) is $\mathcal{O}(m_N^6/\Lambda_{NN}^2 Q^4)$ relative to diagram 2(a) and is expected to dominate the deuteron decay rate. At LO,

$$\Gamma_d|_{\mathcal{Q}_4} = -\kappa(\kappa-\mu)^2\,\mathrm{Im}\,C_0/\pi = -4\kappa^3\,\mathrm{Im}\,a_{np}/m_N \quad (19)$$

in terms of the imaginary part of the $^3S_1$ np scattering length a_{np}. In this case Γ_d^{-1} and $\tau_{n\bar{n}}$ are not dominated by the same $|\Delta B|=2$ LECs, resulting in a larger value of R_d. This implies that if deuteron decay and free n-$\bar{n}$ oscillation are both observed, one could infer whether $|\Delta B|=2$ violation is dominated by $\mathcal{Q}_{1,2,3}$ or by $\mathcal{Q}_4$ (or strangeness-changing operators we have not considered [18, 49]).

In closing, we briefly comment on what our findings imply for heavier nuclei. Due to the low deuteron binding momentum, the expansion in $Q/\Lambda_{NN}\sim\kappa/\Lambda_{NN}$ allows for analytical results. In denser nuclei, such as ^{16}O, this expansion is likely not valid and we need to resum Q/Λ_{NN} corrections by treating pion exchange nonperturbatively. While this complicates the calculations, it only partially affects the power-counting estimates. Contributions from $Q\sim\Lambda_{NN}$ are transferred from LECs to explicit pion exchange. The infrared enhancement by κ^{-1} in the decay rate Eq. (17), which increases the overall sensitivity to $\tau_{n\bar{n}}$, should become less pronounced, but intrinsic two-nucleon effects due to $|\Delta B|=2$ pion exchange and short-range NN annihilation, and $NN\to N\bar{N}$ interactions with unknown LECs appear in the chiral expansion only at N^{2}LO, $\mathcal{O}(Q^2/\Lambda_\chi^2)$, or beyond. Therefore, in conjunction with free n-$\bar{n}$ transitions, stability experiments with denser nuclei also partially discriminate among $|\Delta B|=2$ operators.

BL and UvK thank Z. Chacko for stressing the need for an EFT calculation of the deuteron lifetime. We are also grateful to J. Carbonell and J.-M. Richard for discussions on $N\bar{N}$ potential models. This research was supported by the Dutch Organization for Scientific Research (NWO) under program 156 (FO, RGET), by the National Natural Science Foundation of China (NSFC) through grants Nos. 11735003 and 11775148 (BL), by the U.S. Department of Energy, Office of Science, Office of Nuclear Physics, under award number DE-FG02-04ER41338 (UvK), and by the European Union Research and Innovation program Horizon 2020 under grant agreement No. 654002 (UvK).

[1] S. Weinberg, Phys. Rev. Lett. **43**, 1566 (1979).
[2] S. Weinberg, Phys. Rev. D **22**, 1694 (1980).
[3] H. A. Weldon and A. Zee, Nucl. Phys. B **173**, 269 (1980).
[4] T.-K. Kuo and S. T. Love, Phys. Rev. Lett. **45**, 93 (1980).
[5] K. S. Babu *et al.*, arXiv:1311.5285 [hep-ph].
[6] R. N. Mohapatra and R. E. Marshak, Phys. Rev. Lett. **44**, 1316 (1980) [Erratum: Phys. Rev. Lett. **44**, 1643 (1980)].
[7] J. M. Arnold, B. Fornal, and M. B. Wise, Phys. Rev. D **87**, 075004 (2013).
[8] N. F. Bell, T. Corbett, M. Nee, and M. J. Ramsey-Musolf, arXiv:1808.10597 [hep-ph].
[9] V. A. Kuzmin, Pisma Zh. Eksp. Teor. Fiz. **12**, 335 (1970).
[10] D. G. Phillips II *et al.*, Phys. Rept. **612**, 1 (2016).
[11] M. Baldo-Ceolin *et al.*, Z. Phys. C **63**, 409 (1994).
[12] C. Theroine ($n\bar{n}$ Collaboration), Nucl. Part. Phys. Proc. **273-275**, 156 (2016).
[13] C. Grojean, B. Shakya, J. D. Wells, and Z. Zhang, Phys. Rev. Lett. **121**, 171801 (2018).
[14] P. K. Kabir, Phys. Rev. Lett. **51**, 231 (1983).
[15] B. Aharmim *et al.* (SNO Collaboration), Phys. Rev. D **96**, 092005 (2017).
[16] S. Rao and R. Shrock, Phys. Lett. **116B**, 238 (1982).
[17] W. E. Caswell, J. Milutinovic, and G. Senjanovic, Phys. Lett. **122B**, 373 (1983).
[18] J. Basecq and L. Wolfenstein, Nucl. Phys. B **224**, 21 (1983).
[19] M. I. Buchoff and M. Wagman, Phys. Rev. D **93**, 016005 (2016).
[20] S. Weinberg, Physica A **96**, 327 (1979).
[21] S. Weinberg, Phys. Lett. B **251**, 288 (1990).
[22] A. Manohar and H. Georgi, Nucl. Phys. **B234**, 189 (1984).
[23] F. Oosterhof, MSc Thesis, University of Groningen (2016).
[24] J. Bijnens and E. Kofoed, Eur. Phys. J. C **77**, 867 (2017).
[25] F. Oosterhof, J. de Vries, R. G. E. Timmermans, and U. van Kolck, in preparation.
[26] E. Rinaldi, S. Syritsyn, M. L. Wagman, M. I. Buchoff, C. Schroeder, and J. Wasem, arXiv:1809.00246 [hep-lat].
[27] E. Rinaldi, S. Syritsyn, M. L. Wagman, M. I. Buchoff, C. Schroeder and J. Wasem, arXiv:1901.07519 [hep-lat].
[28] P. F. Bedaque and U. van Kolck, Ann. Rev. Nucl. Part. Sci. **52**, 339 (2002).
[29] D. B. Kaplan, M. J. Savage, and M. B. Wise, Phys. Lett. B **424**, 390 (1998).
[30] D. B. Kaplan, M. J. Savage, and M. B. Wise, Phys. Rev. C **59**, 617 (1999).
[31] M. J. Savage and R. P. Springer, Nucl. Phys. **A686**, 413 (2001).
[32] J. de Vries, E. Mereghetti, R. G. E. Timmermans, and U. van Kolck, Phys. Rev. Lett. **107**, 091804 (2011).
[33] E. Mereghetti, J. de Vries, R. G. E. Timmermans, and U. van Kolck, Phys. Rev. C **88**, 034001 (2013).
[34] S. Fleming, T. Mehen, and I. W. Stewart, Nucl. Phys. **A677**, 313 (2000).
[35] J. J. de Swart, C. P. F. Terheggen, and V. G. J. Stoks, arXiv:nucl-th/9509032.
[36] B. Long, PhD Thesis, University of Arizona (2008).
[37] G. Y. Chen, H. R. Dong, and J. P. Ma, Phys. Lett. B **692**, 136 (2010).
[38] X.-W. Kang, J. Haidenbauer, and U.-G. Meißner, JHEP **02**, 113 (2014).
[39] L.-Y. Dai, J. Haidenbauer, and U.-G. Meißner, JHEP **07**, 078 (2017).
[40] D. Zhou and R. G. E. Timmermans, Phys. Rev. C **86**, 044003 (2012).
[41] D. Zhou and R. G. E. Timmermans, Phys. Rev. C **87**, 054005 (2013).
[42] C. B. Dover, A. Gal, and J.-M. Richard, Phys. Rev. D **27**, 1090 (1983).
[43] P. G. H. Sandars, J. Phys. G **6**, L161 (1980).
[44] J. Carbonell, J.-M. Richard, and S. Wycech, Z. Phys. A **343**, 325 (1992).

[45] J. Arafune and O. Miyamura, Prog. Theor. Phys. **66**, 661 (1981) [Erratum: Prog. Theor. Phys. **66**, 1914 (1981)].
[46] L. A. Kondratyuk, JETP Lett. **64**, 495 (1996).
[47] V. Kopeliovich and I. Potashnikova, JETP Lett. **95**, 1 (2012).
[48] C. B. Dover, A. Gal, and J.-M. Richard, Phys. Rev. C **31**, 1423 (1985).
[49] C. Csaki, Y. Grossman, and B. Heidenreich, Phys. Rev. D **85**, 095009 (2012).